Application of the Transfer Function Approach in the Thermal Analysis of Dynamic Wall Structures

M. Virtanen **I. Heimonen** **R. Kohonen**

ABSTRACT

The transfer function approach (response factor method) for the analysis of dynamic walls is presented. The dynamic wall is understood to be a multilayer porous body through which air flows from outside to inside. Continuity and momentum equations are not solved, i.e., the airflow rate is given as an input value. The wall is assumed to be a one-dimensional dynamic thermal system.

Assuming constant thermal properties for the wall structure and infiltrating air and, in addition, assuming a constant infiltrating airflow rate, the thermal system is linear and the response factor can be applied. For the case where the infiltrating airflow rate is time dependent, an approximation to apply the response factor method is also presented. Comparisons of the results calculated with both the infinite difference method and the response factor method show that the results agree very well with each other.

The implementation of the response factor method to a system simulation program is also considered. An algorithm for solving the heat balance of a building is presented. Also, the effect of dynamic wall structures on the dynamic behavior of a building as well as the heating and cooling load is considered. Energy analyses are done using Denver weather data.

INTRODUCTION

This paper presents the transfer function approach (response factor method) for the analysis of dynamic walls. The dynamic wall is here understood to be a multilayer porous body through which air flows from outside to inside. Heat transfer between the stagnant component (structure) and the flowing component (air) will be considered for one-dimensional dynamic conditions. Continuity and momentum equations are not solved, i.e., the airflow rate is given as an input value of the thermal system.

Starting from the energy equations of a two-component system, the numerical formulation of the heat transfer problem based on the finite-difference method will first be considered. Assuming a constant thermal properties (independent of temperature) of the stagnant and flowing components and, in addition, assuming a constant airflow rate through a structure, the system is linear and the transfer function approach can be applied. For the case where the infiltrating airflow rate varies with time, a transfer function approach will also be presented. The structure level comparisons will show that the results for lightweight and heavyweight dynamic wall structures calculated with the finite-difference method and the response factor method agree very well with each other.

Finally, the implementation of the developed response factor method with a system simulation program will be considered. In the case of dynamic wall structures, the heat balance of the inside surfaces (including the radiative heat transfer) cannot be formed similarly as in the case of airtight structures. Therefore, an alternative solution of room air heat balance is presented. Finally, long-term simulation results of a building with a mechanical exhaust ventilation system and dynamic wall structures (supply air intake) will be shown.

MODEL EQUATIONS

In a two-component system (see Figure 1), the average volume energy equation of the flowing and stagnant component is

$$\frac{\partial\langle\rho_i h_i\rangle}{\partial t} = -\nabla\cdot\langle\vec{q}_i\rangle - \nabla\cdot\langle\rho_i h_i\vec{v}_i\rangle - \frac{1}{V}\sum_j\int_{A_{ij}}\vec{q}_i\cdot\vec{n}_{ij}\,dA \quad (1)$$

$$\frac{\partial\langle\rho_j h_j\rangle}{\partial t} = -\nabla\cdot\langle\vec{q}_j\rangle - \frac{1}{V}\sum_i\int_{A_{ji}}\vec{q}_j\cdot\vec{n}_{ji}\,dA \quad (2)$$

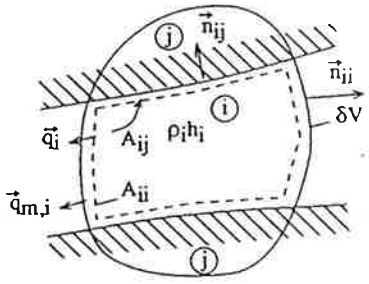

Figure 1 Physical model of a two-component system.

Markku Virtanen is acting research professor, **Ismo Heimonen** is a research scientist, and **Reijo Kohonen** is director, Laboratory of Heating and Ventilation, Technical Research Centre of Finland, Espoo.

Assuming that a local thermodynamic equilibrium exists between the flowing and the stagnant component, i.e., components are locally at the same temperature, Equations 1 and 2 can be combined. If, in addition, heat conduction in the flowing component is omitted, then

$$\frac{\partial(\langle\rho_i h_i\rangle + \langle\rho_j h_j\rangle)}{\partial t} = -\nabla \cdot \langle\rho_i h_i \vec{v}_i\rangle - \nabla \cdot \langle\vec{q}_j\rangle \qquad (3)$$

For the case of homogeneous porous material, where the average volume property is equal to the material property (porosity $e = V_i/V$ = constant, $v = ev_i$, $\rho c_p = (1 - e)\rho_j cp_{,j}, \lambda = (1 - e)\lambda_j$), the one-dimensional form of Equation 3 is

$$\frac{d(\rho h)}{dt} = -\frac{d}{dx}(\rho_i h_i v) - \frac{dq}{dx} \qquad (4)$$

Assuming constant thermal properties, Equation 4 becomes

$$C''' \frac{dT}{dt} = -\dot{C}''_i \frac{dT}{dx} + \lambda \frac{d^2T}{dx^2} \qquad (5)$$

where

$C''' = \rho c_p$,
$\dot{C}_i'' = \rho_i c_{p,i} \cdot v$.

The boundary conditions of the outside and inside surfaces are

$$\alpha_o (T_{eq,o} - T_{s,o}) + \dot{C}''_i T_o = -\lambda\left(\frac{dT}{dx}\right)_o + \dot{C}''_i T_{s,o} \qquad (6)$$

$$-\lambda \left(\frac{dT}{dx}\right)_L + \dot{C}''_i T^* = \alpha_i (T_{s,i} - T_{eq,i}) + \dot{C}''_i T_{s,i} \qquad (7)$$

where T^* is the temperature of the airflow entering the control volume at the interior surface of the structure.

SOLUTION OF ENERGY EQUATIONS WITH FINITE-DIFFERENCE METHOD

If the boundary condition of the first kind for the outside surface of the structure is applied (outside surface at outdoor air temperature), then an analytical solution is possible (Anderlind and Johansson 1980). However, in this paper, Equation 5 is solved numerically for the dynamic condition, applying boundary conditions according to Equations 6 and 7. The numerical formulation of the energy balance equation is done using the finite-difference method. The heat balance equation of an interior grid point n can thus be written:

$$\frac{C'''}{2}(\Delta x\,(n-1) + \Delta x(n))\frac{dT_n}{dt} = \left(\frac{\lambda}{\Delta x\,(n-1)} + \dot{C}''_i\right) T_{n-1} - \left(\frac{\lambda}{\Delta x\,(n-1)} + \frac{\lambda}{\Delta x\,(n)} + \dot{C}''_i\right) T_n + \frac{\lambda}{\Delta x\,(n)} T_{n+1} \qquad (8)$$

The time derivative of temperature T_n in Equation 8 is approximated by the pure implicit method:

$$-2\Delta t \left(\frac{\lambda}{\Delta x(n-1)} + (\dot{C}''_i)^{s+1}\right)T_{n-1}^{s+1} + [C'''(\Delta x\,(n-1) + \Delta x\,(n)) + 2\Delta t\left(\frac{\lambda}{\Delta x(n-1)} + \frac{\lambda}{\Delta x(n)} + (\dot{C}''_i)^{s+1}\right]T_n^{s+1} + 2\Delta t \frac{\lambda}{\Delta x(n)} T_{n-1}^{s+1} = C'''(\Delta x(n-1) + \Delta x\,(n))T_n^s \qquad (9)$$

where superscripts (s) and (s+1) refer to the time increment before and after one calculation time step.

The heat balance equation of exterior surface grid point 1 can be presented in the form

$$\left(\frac{\lambda}{\Delta x(1)} + (\dot{C}''_i)^{s+1} + \alpha_o\right)T_1^{s+1} - \frac{\lambda}{\Delta x(1)} T_2^{s+1} = \alpha_o T_{eq,o}^{s+1} + (\dot{C}''_i)^{s+1} T_o^{s+1} \qquad (10)$$

The heat balance equation of the interior surface grid point N is correspondingly

$$\left(\frac{\lambda}{\Delta x(N-1)} + (\dot{C}''_i)^{s+1}\right)T_{N-1}^{s+1} - \frac{\lambda}{\Delta x(N-1)} + \alpha_i + (\dot{C}''_i)^{s+1})T_N^{s+1} = -\alpha_i T_{eq,i}^{s+1} \qquad (11)$$

Equations 9 through 11 can be written in a matrix form

$$[A]\,(T)^{s+1} = [B]\,(T)^s + (C) \qquad (12)$$

from which the temperatures T_n^{s+1} can be solved.

SOLUTION OF ENERGY EQUATIONS WITH RESPONSE FACTOR METHOD

The transfer function approach (response factor method) (Mitalis and Stephenson 1967) has usually been applied to the calculation of one-dimensional time-dependent conductive heat flows of structures. When applying the method, it is required that the considered thermal system be linear, i.e., the material properties of the structure do not depend on temperature. In the case of a porous body with a constant infiltrating airflow rate through it, the thermal system is also linear, providing the thermal properties of infiltrating air are assumed constant. If the infiltrating airflow rate changes with time, the system is nonlinear. The transfer function approach can be applied, but only as an approximation.

Constant Infiltrating Airflow Rate

In this approach, the conductive heat flow of the interior surface is equal to the convective heat flux:

$$q_{cond,i} = \alpha_i (T_{s,i} - T_{eq,i}) \quad (13)$$

where

α_1 = convective heat transfer coefficient of inside surface,
$T_{s,i}$ = inside surface temperature,
$T_{eq,i}$ = equivalent temperature of indoor air.

It is required that the convective heat transfer coefficient of the interior surface be fixed. In addition, the thermal properties of air and the structural materials are assumed constant.

Response factors of conductive heat flow can be given at (see Figure 2) the

1. outside surface for outside surface temperature excitation, $X_{1,j}$;
2. inside surface for outside surface temperature excitation, $Y_{1,j}$;
3. outside surface for inside air equivalent temperature excitation, $X_{2,j}$;
4. inside surface for inside air equivalent temperature excitation, $Y_{2,j}$.

Defining the positive direction of heat flow from inside to outside, the conductive heat flow of the inside surface is

$$q_{COND,i,n} = \sum_{j=0}^{\infty} Y_{2,j} T_{eq,i,n-j} - \sum_{j=0}^{\infty} Y_{1,j} T_{s,o,n-j} \quad (14)$$

The heat balance equation of the outside surface is

$$\dot{C}_i'' T_{o,n} + \alpha_{o,n} (T_{eq,o,n} - T_{s,o,n}) = \dot{C}_i'' T_{s,o,n} - q_{COND,o,n} \quad (15)$$

and the conductive heat flow of the outside surface is

$$q_{COND,o,n} = \sum_{j=0}^{\infty} X_{2,j} T_{eq,i,n-j} - \sum_{j=0}^{\infty} X_{1,j} T_{s,o,n-j} \quad (16)$$

Combining Equations 15 and 16, the temperature of the outside surface at time $t=n\Delta t$ ($n=1, 2, \ldots$) is obtained:

$$T_{s,o,n} = \frac{\dot{C}_i'' + \alpha_{o,n} T_{eq,o,n} - \sum_{j=1}^{\infty} X_{1,j} T_{s,o,n-j} + \sum_{j=0}^{\infty} X_{2,j} T_{eq,i,n-j}}{\alpha_{o,n} + \dot{C}_i'' + X_{1,o}} \quad (17)$$

Taking Equation 17 into account, the conductive heat flow of the inside surface can be calculated using Equation 14.

It is assumed that the infiltrating air enters the room space at the interior surface temperature of a structure (upwind scheme) and the corresponding airflow rate leaves the room space at the indoor air temperature. In other words, the control surface of room air is at the inside surface of structures. Thus the convective heat flow of infiltrating air is

$$q_{CONV,n} = \dot{C}_i'' (T_{i,n} - T_{s,i,n}), \dot{C}_i'' \geq 0 \quad (18)$$

where

$\dot{C}_i''$ = heat capacity flow rate/unit surface,
$T_{i,n}$ = indoor air temperature,
$T_{s,i,n}$ = interior surface temperature of a structure.

Time-Dependent Infiltrating Airflow Rate

In the previous section, a porous body with a constant infiltrating airflow rate was considered. In addition, constant thermal properties were assumed, i.e., in this case the thermal system was linear, which is required when applying the response factor method. Due to the nonlinearity of varying airflow rate, an approximation is needed. The approximation is illustrated in Figure 3.

The sum of response factors at the inside surface of a structure for outside surface temperature excitation must be equal to the sum of response factors for inside air equivalent temperature excitation in order to reach the thermal

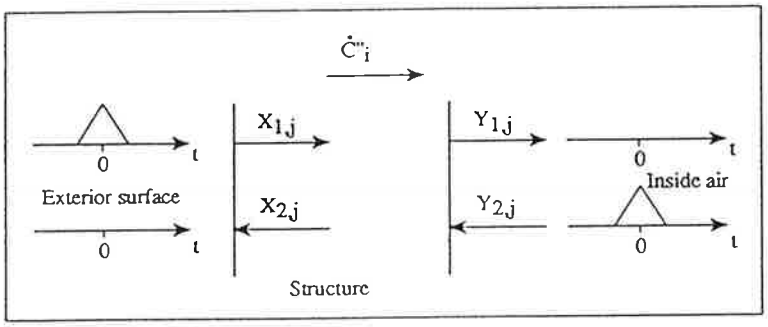

Figure 2 Response factors with constant airflow rate.

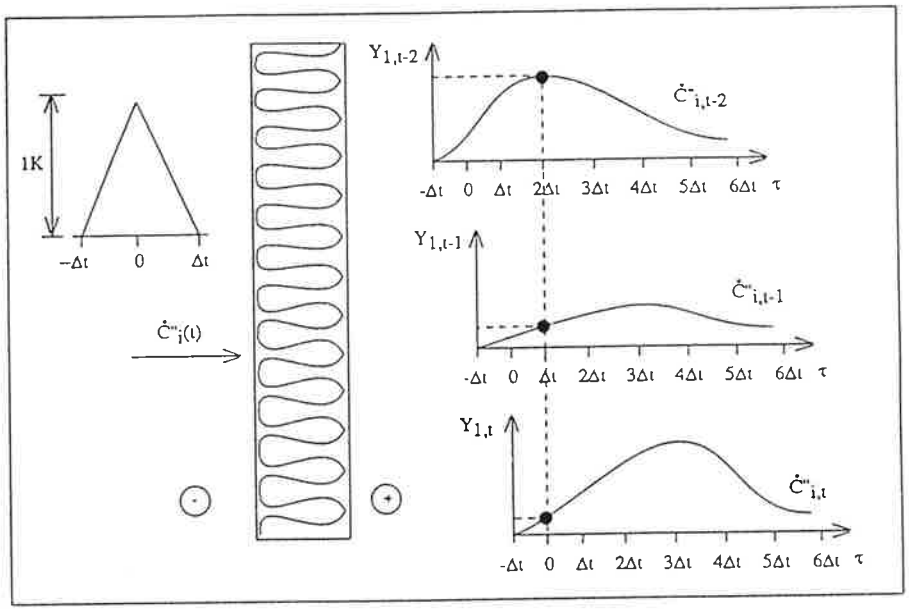

Figure 3 *Response of inside surface conduction heat flow for outside surface temperature excitation in a case of varying airflow rate.*

balance. Also, the response factors at the outside surface must obey the same rule. The following correction to response factors $Y_{1,j}$ and $X_{2,j}$ at every time step is done if the airflow rate is changed:

$$\begin{cases} Y^{c}_{1,j,n-j} = Y_{1,j,n-j} \dfrac{\sum_{j=0}^{\infty} Y_{2,j,n-j}}{\sum_{j=0}^{\infty} Y_{1,j,n-j}} \\ X^{c}_{2,j,n-j} = X_{2,j,n-j} \dfrac{\sum_{j=0}^{\infty} X_{1,j,n-j}}{\sum_{j=0}^{\infty} X_{2,j,n-j}} \end{cases} \quad (19)$$

where C refers to a corrected value.

Thus the conductive heat flow of the inside surface (Equation 14) is approximated in the following way:

$$q_{COND,i,n} = \sum_{j=0}^{\infty} Y_{2,j,n-j}\, T_{eq,i,n-j} - \sum_{j=0}^{\infty} Y_{1,j,n-j}\, T_{s,o,n-j} \quad (20)$$

The corresponding approximation of the outside surface temperature (Equation 17) is

$$T_{s,o,n} = \frac{C_{i,n}\, T_{o,n} + \alpha_{o,n}\, T_{eq,o,n} - \sum_{j=1}^{\infty} X_{1,j,n-j}\, T_{s,o,n-j} + \sum_{j=0}^{\infty} X^{c}_{2,j,n-j}\, T_{eq,i,n-j}}{\alpha_{o,n} + C_{i,n} + X_{1,o,n}} \quad (21)$$

The convective heat flow of the infiltrating air is calculated using Equation 18.

COMPARISON OF RESULTS CALCULATED WITH THE RESPONSE FACTOR METHOD AND FINITE-DIFFERENCE METHOD

Two dynamic wall structures were chosen for comparative studies. Property values used in the calculation are given in Table 1. With the two structures, two different cases are considered. In these, outside air temperature, equivalent outside temperature, inside air temperature, and the capacity flow rate of infiltrating air are changing periodically with time, as shown in Figure 4. The radiative heat transfer at the interior surface has been neglected in the calculations.

The calculation time step using the finite-difference method was five minutes. When using the response factor method, the calculation time step was one hour. Response

TABLE 1
Thermal Properties of the Dynamic Wall Structures

	Lightweight structure	Heavyweight structure
thermal conductivity	0.04 W/mK	0.08 W/mK
heat capacity	850 J/kgK	850 J/kgK
density	40 kg/m³	400 kg/m³
thickness	72 mm	145 mm
interior convective heat transfer coefficient	8.35 W/m²K	8.35 W/m²K
exterior convective heat transfer coefficient	17.0 W/m²K	17.0 W/m²K

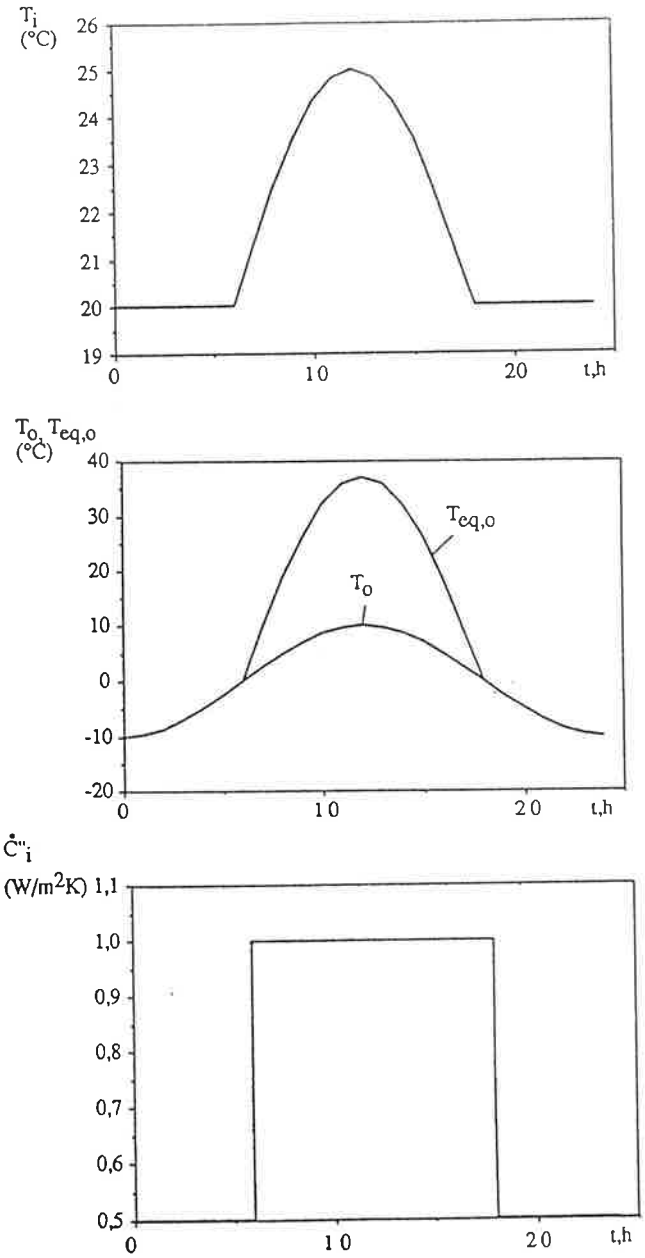

Figure 4 *Inside air temperature, outside air temperature, equivalent outside temperature, and heat capacity flow rate in comparative calculations.*

factors (see Appendix A) were calculated using the finite-difference method with a one-minute time step. As the response factors were determined, the temperature profiles of exterior surface and inside air were as illustrated in Figure 2.

The conductive heat flow at the interior surface of a lightweight structure and the convective heat flow of infiltrating air are shown in Figure 5. The corresponding results for a heavyweight structure are shown in Figure 6.

In general, it can be concluded that, in both wall structures, the results calculated with the finite-difference and response factor methods agree very well with each

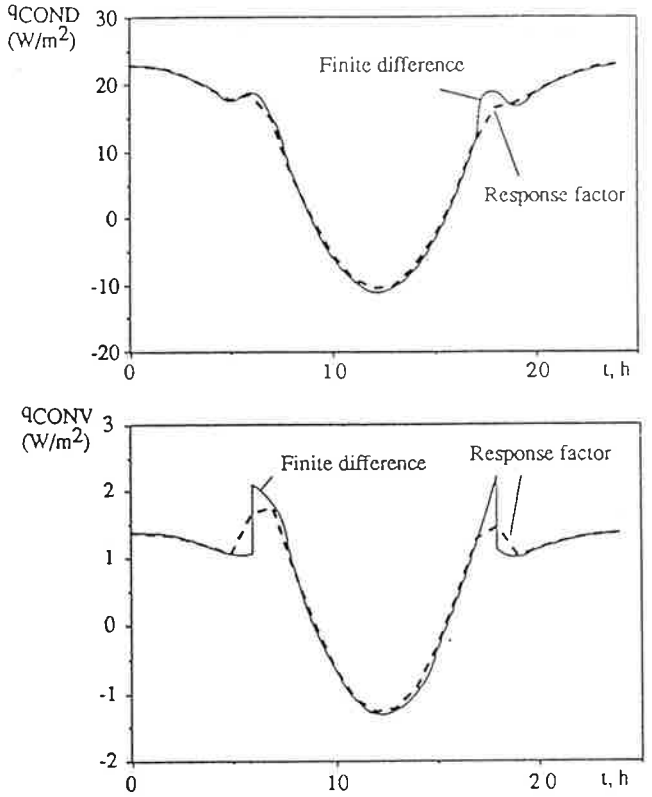

Figure 5 *The conductive heat flow at interior surface and the convective heat flow in a case of a lightweight structure.*

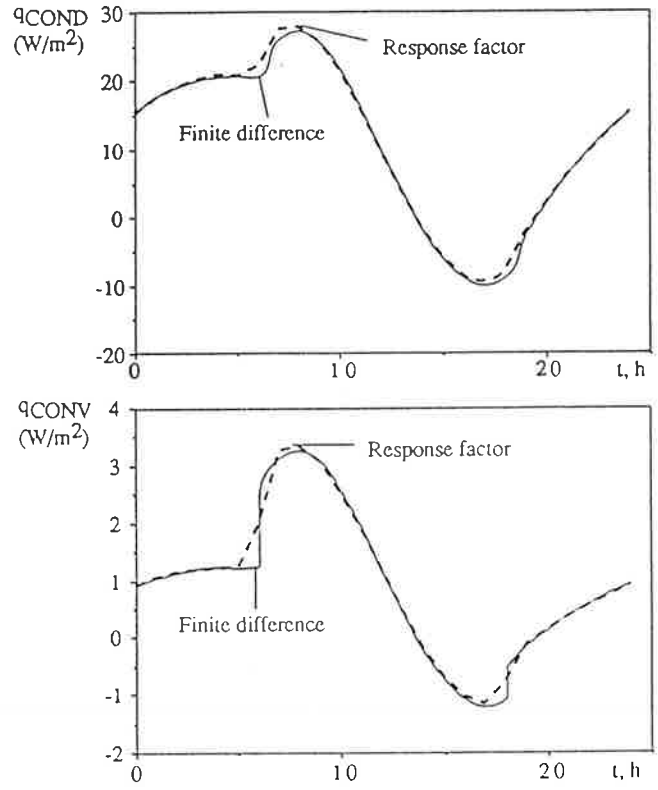

Figure 6 *The conductive heat flow at interior surface and the convective heat flow in a case of a heavyweight structure.*

other. The only differences seem to be due to the different calculation time step. Also, in the case of the heavyweight structure, the delay of conductive heat flow at the interior surface using the response factor method is smaller than the delay using the finite-difference method when the infiltrating airflow rate is changing rapidly. This difference is clearly due to the approximative method to apply response factors in a nonlinear thermal system.

COUPLING OF THE RESPONSE FACTOR METHOD WITH ZONE MODEL

Solution of the Heat Balance of a Building

In the following, the application of the present response factor method in a building heat balance analysis will be considered. In general, the problem now is that the heat balance for a single inside surface of the dynamic wall structure cannot be formed in a conventional way. The surface temperatures have to be solved iteratively. By considering a convective heat balance model of a building (zone model), as shown in Figure 7, the heat balance of a room space is in a dynamic condition:

$$C_i \frac{dT_i}{dt} = -(\phi_w + \phi_c + \phi_f + \phi_{wi}) - (\dot{C}_i T_i - \dot{C}_i T_i - \dot{C}_i T_{s,i}) + (\phi_H + \phi_P + \phi_L) \quad (22)$$

which reduces to

$$C_i \frac{dT_i}{dt} = -\sum \phi_{cond} - \phi_{conv} + \sum \phi_H \quad (23)$$

In the heat balance, the radiant heat transfer between inside surfaces should also be taken into account. This can be done by the introduction of equivalent room air temperature to each isothermal surface:

$$(T_{eq,i})_k = T_i + (q_{r,k} + \sum_l \alpha_{r,k} ((T_{s,i})_l - (T_{s,i})_k))/\alpha_{i,k} \quad (24)$$

where

k	=	a considered surface;
l	=	surrounding surfaces;
$q_{r,k}$	=	the sum of radiative gains absorbed by the surface from solar radiation, lights, etc.;
$\alpha_{r,k}$	=	the radiative heat transfer coefficient;
$\alpha_{l,k}$	=	the convective heat transfer coefficient.

Equation 23 can be written in the form

$$C_i \frac{dT_i}{dt} = -\sum_k \alpha_{i,k} A_k (T_i - (T_{s,i})_k) - (\dot{C}_i T_i - \sum_k \dot{C}_{i,k} A_k (T_{s,i})_k) + \sum \phi_H \quad (25)$$

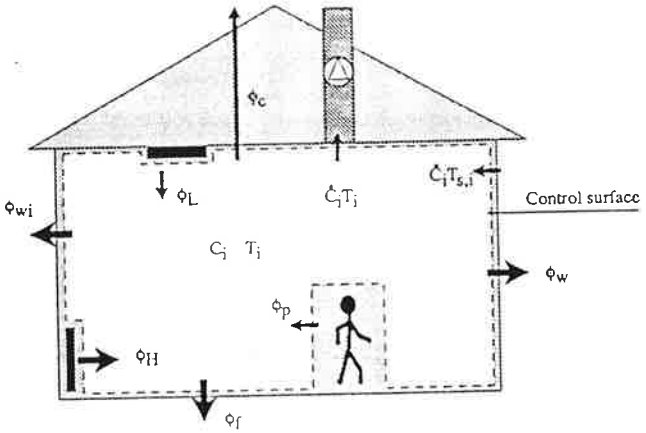

Figure 7 Convective heat balance of a building.

An implicit discrete form of Equation 25 is

$$C_i \frac{T_{i,t} - T_{i,t-\Delta t}}{\Delta t} = -\sum_k \alpha_{i,k} A_k (T_i - (T_{s,i})_k) - (\dot{C}_i T_i - \sum_k \dot{C}_i A_k (T_{s,i})_k) + \sum \phi_H \quad (26)$$

where the terms on the right-hand side are average values during the time step Δt.

The average inside air temperature is

$$T_i = \frac{T_{i,t} + T_{i,t-\Delta t}}{2} \quad (27)$$

Substituting Equation 27 into Equation 26 becomes

$$(\frac{2C_i}{\Delta t} + \sum_k \alpha_{i,k} A_k + \dot{C}_i) T_i = \sum_k \alpha_{i,k} A_k (T_{s,i})_k + \sum_k \dot{C}_{i,k} A_k (T_{s,i})_k + \sum \phi_H + \frac{2C_i}{\Delta t} T_{i,t-\Delta t} \quad (28)$$

The inside air temperature T_i (average) is solved by double iteration. The solution algorithm is, in principle, as follows (K refers to the number of isothermal inside surfaces):

1. Guess inside air temperature, T_i.
2. Guess $(T_{eq,i})_{k=1,...K}$.
3. Solve $(T_{s,o})_{k=1,...K}$ using Equation 17 or 21.
4. Solve conductive heat flows of interior surfaces using Equation 14 or 19.
5. Solve surface temperatures:

$$(T_{s,i})_{k=1,...k} = [(T_{eq,i})_k + (q_i)_k/\alpha_{i,k}]_{k=1,...k} \quad (29)$$

6. Solve net radiative heat flows of surfaces:

$$(q_{r,net})_k = [q_{r,k} + \sum_l \alpha_{r,k}((T_{s,i})_l - (T_{s,i})_k]_{k=1,...k} \quad (30)$$

TABLE 2
Short-Term Simulation Cases

Case	Excitation	Description
1	Outdoor air temperature	Outdoor air temperature changes from 20°C to 21°C instantly at time 48 hours.
2	Outer surface radiation	Radiation to external surfaces (east and west) changes from 0 W/m² to 600 W/m² instantly at time 48 hours. Outdoor air temperature is 20°C.
3	Internal convective gain	Internal convective gain changes from 0 W to 600 W instantly at time 48 hours. Outdoor air temperature is 20°C.
4	Infiltration air flow rate	Air change rate of the building changes from 0 to 0,5 ach at time 48 hours and from 0,5 to 1,0 ach at time 72 hours. Internal convective gain is 2000 W. Outdoor air temperature is 0°C.

7. Calculate $(T_{eq,i})_{k=1,...k}^{new}$ using Equation 24.

   Test, if $[(T_{eq,i})_k^{new} - (T_{eq,1})_k] > \varepsilon_1 \rightarrow 2°$.
8. Solve T_i^{new} using Equation 28.
   Test, if $[T_i^{new} - T_i] > \varepsilon_2 \rightarrow 1°$.

The present zone model has been implemented to a system simulation program (EES 1988).

Short-Term Test Simulations

Test simulations for the new zone model have been done with the "shoebox" building of IEA Task 13 (IEA, n.d.). The characteristics of the building are described in Appendix B. In test simulations, both heavyweight and lightweight structures, as well as different air change rates of the building, have been considered. The building is supplied with an exhaust ventilation system, where the supply air is taken in either through porous dynamic wall structures (heat recovery effect taken into account) or through inlet devices where the supply air flows in at the outside air temperature.

For different test cases, described in Table 2, the building is affected by internal or external excitations that in the present cases are outdoor air temperature, internal convective heat gain, external radiative gain, and air change rate. As the supply air is taken in through the dynamic wall structures, it should be noticed that only the east and west walls of the building are porous dynamic wall structures.

In case 1 (see Figure 8), the outdoor air temperature changes from 20°C to 21°C at 48 hours. Internal gains are zero, and only lightweight structures are considered. Both for the case where supply air is taken in through porous dynamic walls and where it is taken in at outdoor air temperature, the response of indoor air becomes faster when the air change rate of the building is increased. On the other hand, it should be noticed that the effect of outdoor air temperature excitation on room air temperature is overestimated if the thermal coupling of infiltrating air

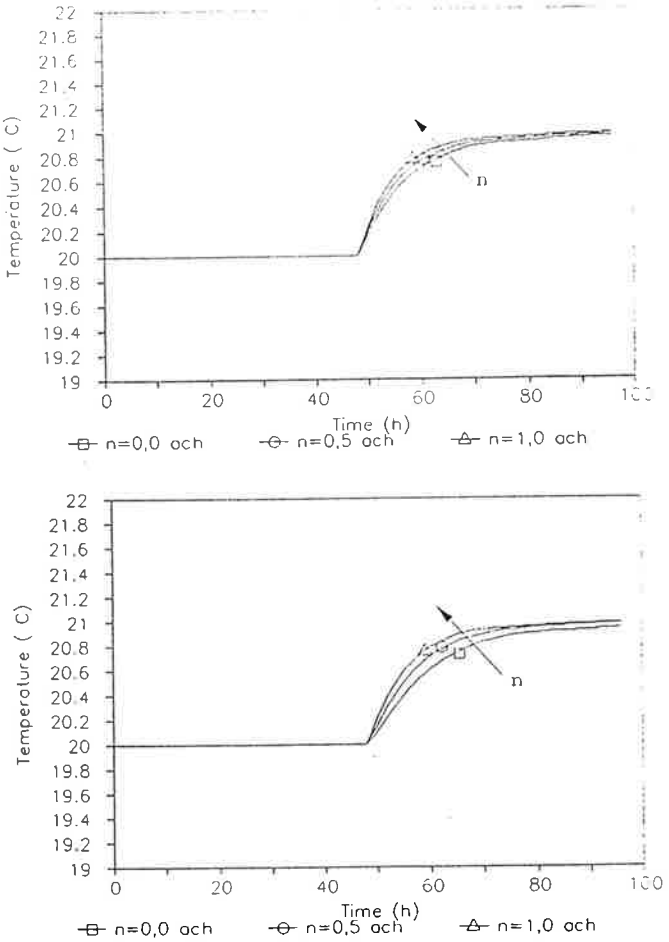

Figure 8 *Room air temperature response for outdoor air temperature excitation in a case of a light-weight structure. Upper curve is for dynamic walls and lower curve is for airtight walls.*

and wall structures is not taken into account. If the supply air flows in at outdoor air temperature, the effect of air change rate on room air temperature response is greater than in the dynamic wall structure case.

In case 2, the solar radiation to the eastern and western external surfaces changes instantly from zero to 600 W/m² at 48 hours (see Figure 9). Outdoor air temperature is constant at 20°C. When using dynamic wall structures, the response of inside air temperature for the radiation gain on external surfaces is faster than where the supply air is taken in at outdoor air temperature. Also, the effect of air change rate on the inside temperature behavior is opposite these two air intake arrangements. External surface radiation quickly affects the temperature of infiltrating air through the porous body. The larger the infiltration airflow rate, the higher and faster is the rise of the indoor air temperature. If the supply air is taken in at the outside air temperature, i.e., the heat transfer between airflow and structure is omitted, the increase of ventilation rate lowers the room air temperature closer to the outdoor air temperature.

In case 3, only the internal convective gain changes instantly from zero to 600 W at 48 hours with constant

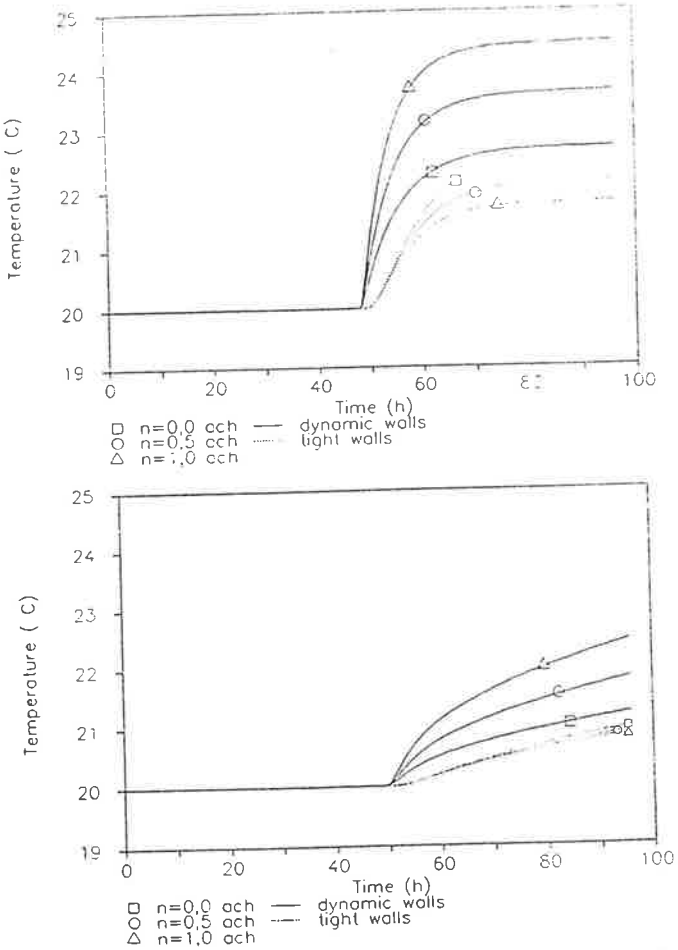

Figure 9 *Room air temperature response for external surface power excitation. Upper case is lightweight structures and lower case is heavyweight structures.*

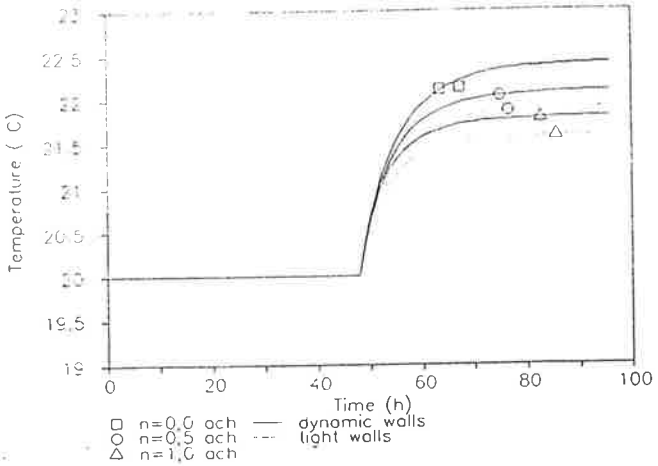

Figure 10 *Room air temperature response for infiltration airflow rate excitation. Lightweight and heavyweight structures.*

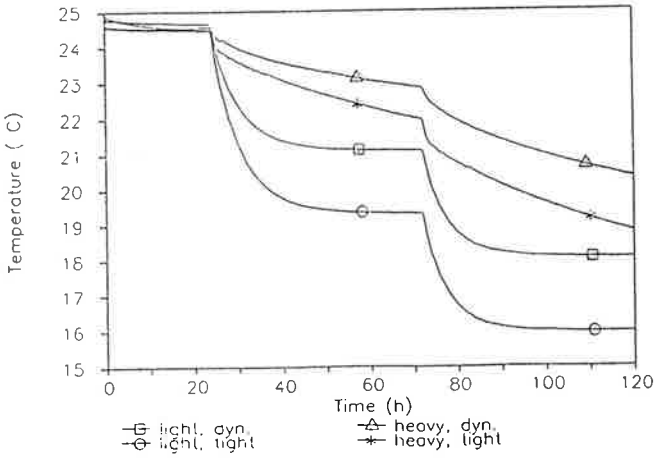

Figure 11 *Room air temperature response for infiltration airflow rate excitation. Lightweight and heavyweight structures.*

20°C outdoor air temperature and lightweight structures. It can be concluded from Figure 10 that in the case of porous dynamic wall structures, the effect of convective gain on the indoor air temperature is stronger than the case where supply air flows in at outdoor air temperature because the cooling effect of outdoor air is smaller. Increasing the air change rate also increases the cooling effect in both cases. The effect of internal radiative gains is very similar to the effect of convective gains.

In case 4, the air change rate changes from zero to 0.5 ach at 48 hours and from 0.5 ach to 1.0 ach at 72 hours, respectively. Internal convective gain is 2,000 W and outdoor air temperature is 0°C. It can be seen from Figure 11 that the response of indoor air temperature is much faster in lightweight cases than in heavyweight cases. As mentioned above, the cooling effect of ventilation is stronger if the supply air is taken in at the outdoor air temperature instead of using dynamic wall structures.

Long-Term Simulations

In order to illustrate the effect of dynamic wall structures on the annual energy consumption of the "shoebox" building, long-term simulations were carried out with Denver weather data. The room air temperature of the building was allowed to vary in the range 20-27°C.

For the energy analyses, two cases were selected. In case 1 the ventilation rate of the building is 1 ach all day and the supply air of the exhaust ventilation system is taken in at the outdoor air temperature. In case 2 the ventilation rate is similarly 1 ach all day, but the supply air is taken in through eastern and western dynamic wall structures. Both lightweight and heavyweight structures were considered.

The results of the long-term simulations are shown in Table 3. From the results it can be concluded that in case 2 the heating load with lightweight structures is 8% less than in case 1. With heavyweight structures, the corresponding difference is 18%. On the other hand, when using dynamic wall structures the cooling load is increased. With lightweight and heavyweight wall structures, the cooling load is increased 14% and 19%, respectively.

TABLE 3
Results of Long-Term Simulations

Case	Heating load (kWh)	Cooling load (kWh)	Ventilation loss (kWh)
1, lightweight	7516	4110	-4111
1, heavyweight	4528	1147	-4153
2, lightweight	6899	4703	-178
2, heavyweight	3729	1368	-187

CONCLUSIONS

The response factor method for the thermal analysis of dynamic walls has been presented. The inflowing airflow rate of dynamic walls was given as an input value, and the structure was considered as a one-dimensional thermal system. By assuming constant thermal properties of a structure and infiltrating air and, in addition, assuming a constant infiltrating airflow rate, the system is linear and the response factor method can be applied directly. For the cases where the infiltrating airflow rate is time dependent, an approximation for the original response factor method was developed. Comparisons of the results calculated for lightweight and heavyweight dynamic wall structures with both the finite-difference method and the response factor method showed that the results agree very well with each other.

The coupling of the response factor method with the solution of the heat balance of a building was also presented. The solution algorithm based on double iteration was presented. A new zone model has been implemented to a system simulation program.

By short-term test simulations, the effect of dynamic walls on the dynamic behavior of room air temperature was considered. In these considerations, the supply air of a mechanical exhaust ventilation system was taken in either through dynamic walls or through inlet devices where the supply air flows in at the outside temperature. The short-term simulations showed clearly that, when using dynamic walls for supply air intake, the response of room air temperature to the excitation of outdoor air temperature, solar radiation, and the internal convective and radiative heat gains was significantly different than the case where the supply air was taken in at outdoor air temperature. When using dynamic walls, the room air temperature reacted more slowly to changes in outdoor air temperature and faster to solar radiation and internal heat gains.

Finally, the long-term simulations showed a significant decrease of heating energy consumption and an increase of cooling energy consumption in cases where the supply air of the exhaust ventilation system was taken in through dynamic wall structures. According to simulation results, it is evident that in order to prevent overheating during the cooling season, solar shielding for dynamic walls should be used.

ACKNOWLEDGMENT

This work has been financially supported by the Ministry of Trade and Industry of Finland through the Energy Efficient Buildings and Building Components research program. The work has been done within the framework of the International Energy Agency/Solar Heating and Cooling Program. The system simulation program used was TRNSYS.

NOMENCLATURE

A	=	surface area, m^2
C	=	heat capacity, J/K
$\dot{C}''$	=	heat capacity flow rate/unit surface, $W/m^2 \cdot K$
C''	=	heat capacity/unit volume, $J/m^3 \cdot K$
c_p	=	specific heat capacity, $J/kg \cdot K$
h	=	specific enthalpy, J/kg
$\bar{n}_{ij}$	=	unit normal vector of the interfacial surface
q	=	heat flux, W/m^2
T	=	temperature, °C
t	=	time, s, h
T_s	=	surface temperature, °C
T_{eq}	=	equivalent air temperature, °C
T^*	=	temperature of airflow entering the control volume of the interior surface of the structure, °C
V	=	volume, m^3
v	=	velocity, $m \cdot s^{-1}$
x	=	space coordinate, m
X_1, X_2, Y_1, Y_2	=	response factors, $W/m^2 \cdot K$
ϕ	=	heat flow, W
α	=	convective heat transfer coefficient, $W/m^2 \cdot K$
α_r	=	radiative heat transfer coefficient, $W/m^2 \cdot K$
λ	=	thermal conductivity, $W/m \cdot K$
ρ	=	density, kg/m^3

Subscripts

o	=	outside
i	=	inside
r	=	radiative
cond	=	conductive
conv	=	convective

$$\langle b \rangle = \frac{1}{V} \int_{V_i} b_i \, dV$$

REFERENCES

Anderlind, G., and B. Johansson. 1980. Dynamisk isolering. Teori för värmeisolering som genomströmmas av gas eller vätska. Byggforskningsrådet, Rapport R 162:1980. Stockholm.

EES (Engineering Experiment Station). 1988. Report 38-12. A transient system simulation program. Solar Energy Laboratory, University of Wisconsin-Madison. 194 pages.

IEA. n.d. Specification for IEA VIII design tool evaluation exercise. Appendix A. 11 pages.

Mitalas, G.P., and D.G. Stephenson. 1967. Room thermal response factors. *ASHRAE Transactions* 73(1). Atlanta: American Society of Heating, Refrigerating and Air-Conditioning Engineers, Inc.

APPENDIX A

RESPONSE FACTORS OF DYNAMIC WALL STRUCTURES AS HEAT CAPACITY FLOW RATE PER UNIT SURFACE AS A PARAMETER VALUE

Heavyweight structure

X1, W/(m²K)

j	0.0 W/m²K	0.5 W/m²K	1.0 W/m²K
0	2.77190	2.56508	2.37415
1	-1.49114	-1.50441	-1.50397
2	-0.29660	-0.29544	-0.28578
3	-0.15352	-0.15152	-0.14289
4	-0.09631	-0.09403	-0.08632
5	-0.06502	-0.06264	-0.05587
6	-0.04511	-0.04282	-0.03705
7	-0.03160	-0.02953	-0.02477
8	-0.02222	-0.02043	-0.01661
9	-0.01564	-0.01415	-0.01114
10	-0.01101	-0.00980	-0.00748
11	-0.00775	-0.00679	-0.00502
12	-0.00546	-0.00471	-0.00337
13	-0.00385	-0.00326	-0.00226
14	-0.00271	-0.00226	-0.00152
15	-0.00191	-0.00157	-0.00102
16	-0.00134	-0.00109	-0.00069
17	-0.00095	-0.00075	-0.00046
18	-0.00067	-0.00052	-0.00031
19	-0.00047	-0.00036	-0.00021
20	-0.00033	-0.00025	-0.00014
21	-0.00023	-0.00017	-0.00009
22	-0.00016	-0.00012	-0.00006
23	-0.00012	-0.00008	-0.00004
24	-0.00008	-0.00006	-0.00003
25	-0.00006	-0.00004	-0.00002
26	-0.00004	-0.00003	-0.00001
27	-0.00003	-0.00002	-0.00001
28	-0.00002	-0.00001	-0.00001
29	-0.00001	-0.00001	0.00000

X2, W/(m²K)

j	0.0 W/m²K	0.5 W/m²K	1.0 W/m²K
0	0.00071	0.00051	0.00037
1	0.03198	0.02172	0.01465
2	0.09443	0.06145	0.03934
3	0.10221	0.06440	0.03940
4	0.08193	0.05042	0.02970
5	0.06018	0.03632	0.02067
6	0.04300	0.02549	0.01404
7	0.03043	0.01774	0.00946
8	0.02147	0.01231	0.00636
9	0.01513	0.00854	0.00427
10	0.01066	0.00592	0.00287
11	0.00751	0.00410	0.00193
12	0.00529	0.00284	0.00129
13	0.00372	0.00197	0.00087
14	0.00262	0.00136	0.00058
15	0.00185	0.00095	0.00039
16	0.00130	0.00066	0.00026
17	0.00092	0.00045	0.00018
18	0.00065	0.00031	0.00012
19	0.00045	0.00022	0.00008
20	0.00032	0.00015	0.00005
21	0.00023	0.00010	0.00004
22	0.00016	0.00007	0.00002
23	0.00011	0.00005	0.00002
24	0.00008	0.00003	0.00001
25	0.00006	0.00002	0.00001
26	0.00004	0.00002	0.00000
27	0.00003	0.00001	0.00000
28	0.00002	0.00001	0.00000
29	0.00001	0.00001	0.00000

Y1, W/(m²K)

j	0.0 W/m²K	0.5 W/m²K	1.0 W/m²K
0	0.00071	0.00125	0.00210
1	0.03198	0.05269	0.08305
2	0.09443	0.14909	0.22302
3	0.10221	0.15625	0.22338
4	0.08193	0.12232	0.16834
5	0.06018	0.08812	0.11717
6	0.04300	0.06185	0.07958
7	0.03043	0.04305	0.05364
8	0.02147	0.02987	0.03606
9	0.01513	0.02071	0.02422
10	0.01066	0.01435	0.01626
11	0.00751	0.00995	0.01092
12	0.00529	0.00689	0.00733
13	0.00372	0.00478	0.00492
14	0.00262	0.00331	0.00330
15	0.00185	0.00229	0.00222
16	0.00130	0.00159	0.00149
17	0.00092	0.00110	0.00100
18	0.00065	0.00076	0.00067
19	0.00045	0.00053	0.00045
20	0.00032	0.00037	0.00030
21	0.00023	0.00025	0.00020
22	0.00016	0.00018	0.00014
23	0.00011	0.00012	0.00009
24	0.00008	0.00008	0.00006
25	0.00006	0.00006	0.00004
26	0.00004	0.00004	0.00003
27	0.00003	0.00003	0.00002
28	0.00002	0.00002	0.00001
29	0.00001	0.00001	0.00001

Y2, W/(m²K)

j	0.0 W/m²K	0.5 W/m²K	1.0 W/m²K
0	2.13876	2.29679	2.45435
1	-0.93005	-0.89031	-0.84349
2	-0.25880	-0.24381	-0.22310
3	-0.14004	-0.13055	-0.11632
4	-0.08938	-0.08234	-0.07136
5	-0.06073	-0.05518	-0.04644
6	-0.04223	-0.03780	-0.03085
7	-0.02961	-0.02609	-0.02064
8	-0.02082	-0.01806	-0.01384
9	-0.01466	-0.01251	-0.00929
10	-0.01032	-0.00866	-0.00624
11	-0.00727	-0.00600	-0.00419
12	-0.00512	-0.00416	-0.00281
13	-0.00361	-0.00288	-0.00189
14	-0.00254	-0.00200	-0.00127
15	-0.00179	-0.00138	-0.00085
16	-0.00126	-0.00096	-0.00057
17	-0.00089	-0.00066	-0.00038
18	-0.00062	-0.00046	-0.00026
19	-0.00044	-0.00032	-0.00017
20	-0.00031	-0.00022	-0.00012
21	-0.00022	-0.00015	-0.00008
22	-0.00015	-0.00011	-0.00005
23	-0.00011	-0.00007	-0.00004
24	-0.00008	-0.00005	-0.00002
25	-0.00005	-0.00004	-0.00002
26	-0.00004	-0.00002	-0.00001
27	-0.00003	-0.00002	-0.00001
28	-0.00002	-0.00001	0.00000
29	-0.00001	-0.00001	0.00000

Lightweight structure

X1, W/(m²K)

j	0.0 W/m²K	0.5 W/m²K	1.0 W/m²K
0	0.74229	0.53567	0.38649
1	-0.21900	-0.21199	-0.19454
2	-0.00173	-0.00173	-0.00173
3	-0.00040	-0.00041	-0.00042
4	-0.00014	-0.00014	-0.00015
5	-0.00006	-0.00006	-0.00006
6	-0.00003	-0.00003	-0.00003
7	-0.00001	-0.00001	-0.00001
8	-0.00001	-0.00001	-0.00001
9	0.00000	0.00000	0.00000
10	0.00000	0.00000	0.00000
11	0.00000	0.00000	0.00000
12	0.00000	0.00000	0.00000
13	0.00000	0.00000	0.00000
14	0.00000	0.00000	0.00000
15	0.00000	0.00000	0.00000
16	0.00000	0.00000	0.00000
17	0.00000	0.00000	0.00000
18	0.00000	0.00000	0.00000
19	0.00000	0.00000	0.00000
20	0.00000	0.00000	0.00000
21	0.00000	0.00000	0.00000
22	0.00000	0.00000	0.00000
23	0.00000	0.00000	0.00000
24	0.00000	0.00000	0.00000
25	0.00000	0.00000	0.00000
26	0.00000	0.00000	0.00000
27	0.00000	0.00000	0.00000
28	0.00000	0.00000	0.00000
29	0.00000	0.00000	0.00000

X2, W/(m²K)

j	0.0 W/m²K	0.5 W/m²K	1.0 W/m²K
0	0.40272	0.25108	0.15058
1	0.11809	0.07019	0.03896
2	0.00010	0.00004	0.00001
3	0.00000	0.00000	0.00000
4	0.00000	0.00000	0.00000
5	0.00000	0.00000	0.00000
6	0.00000	0.00000	0.00000
7	0.00000	0.00000	0.00000
8	0.00000	0.00000	0.00000
9	0.00000	0.00000	0.00000
10	0.00000	0.00000	0.00000
11	0.00000	0.00000	0.00000
12	0.00000	0.00000	0.00000
13	0.00000	0.00000	0.00000
14	0.00000	0.00000	0.00000
15	0.00000	0.00000	0.00000
16	0.00000	0.00000	0.00000
17	0.00000	0.00000	0.00000
18	0.00000	0.00000	0.00000
19	0.00000	0.00000	0.00000
20	0.00000	0.00000	0.00000
21	0.00000	0.00000	0.00000
22	0.00000	0.00000	0.00000
23	0.00000	0.00000	0.00000
24	0.00000	0.00000	0.00000
25	0.00000	0.00000	0.00000
26	0.00000	0.00000	0.00000
27	0.00000	0.00000	0.00000
28	0.00000	0.00000	0.00000
29	0.00000	0.00000	0.00000

Y1, W/(m²K)

j	0.0 W/m²K	0.5 W/m²K	1.0 W/m²K
0	0.40272	0.60554	0.84393
1	0.11809	0.16928	0.21833
2	0.00010	0.00010	0.00007
3	0.00000	0.00000	0.00000
4	0.00000	0.00000	0.00000
5	0.00000	0.00000	0.00000
6	0.00000	0.00000	0.00000
7	0.00000	0.00000	0.00000
8	0.00000	0.00000	0.00000
9	0.00000	0.00000	0.00000
10	0.00000	0.00000	0.00000
11	0.00000	0.00000	0.00000
12	0.00000	0.00000	0.00000
13	0.00000	0.00000	0.00000
14	0.00000	0.00000	0.00000
15	0.00000	0.00000	0.00000
16	0.00000	0.00000	0.00000
17	0.00000	0.00000	0.00000
18	0.00000	0.00000	0.00000
19	0.00000	0.00000	0.00000
20	0.00000	0.00000	0.00000
21	0.00000	0.00000	0.00000
22	0.00000	0.00000	0.00000
23	0.00000	0.00000	0.00000
24	0.00000	0.00000	0.00000
25	0.00000	0.00000	0.00000
26	0.00000	0.00000	0.00000
27	0.00000	0.00000	0.00000
28	0.00000	0.00000	0.00000
29	0.00000	0.00000	0.00000

Y2, W/(m²K)

j	0.0 W/m²K	0.5 W/m²K	1.0 W/m²K
0	0.70473	0.94233	1.20620
1	-0.18325	-0.16690	-0.14340
2	-0.00047	-0.00043	-0.00039
3	-0.00007	-0.00007	-0.00007
4	-0.00002	-0.00002	-0.00002
5	-0.00001	-0.00001	-0.00001
6	0.00000	0.00000	0.00000
7	0.00000	0.00000	0.00000
8	0.00000	0.00000	0.00000
9	0.00000	0.00000	0.00000
10	0.00000	0.00000	0.00000
11	0.00000	0.00000	0.00000
12	0.00000	0.00000	0.00000
13	0.00000	0.00000	0.00000
14	0.00000	0.00000	0.00000
15	0.00000	0.00000	0.00000
16	0.00000	0.00000	0.00000
17	0.00000	0.00000	0.00000
18	0.00000	0.00000	0.00000
19	0.00000	0.00000	0.00000
20	0.00000	0.00000	0.00000
21	0.00000	0.00000	0.00000
22	0.00000	0.00000	0.00000
23	0.00000	0.00000	0.00000
24	0.00000	0.00000	0.00000
25	0.00000	0.00000	0.00000
26	0.00000	0.00000	0.00000
27	0.00000	0.00000	0.00000
28	0.00000	0.00000	0.00000
29	0.00000	0.00000	0.00000

APPENDIX B

SHOEBOX BUILDING DESCRIPTION WITH DYNAMIC EAST AND WEST WALLS

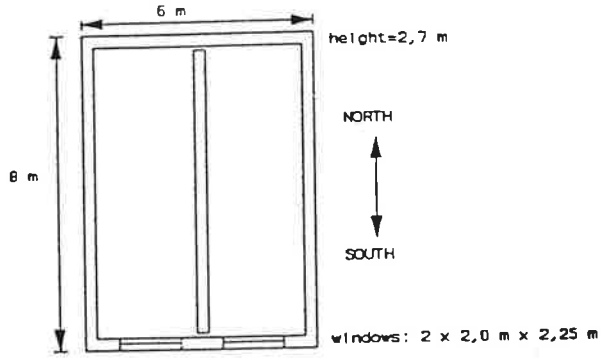

Structure	Layers	Thickness (m)	Conductivity (W/mK)	Density (kg/m^3)	Specific heat capacity (J/kgK)	Resistance (m^{2}K/W)
Lightweight wall, tight	plasterboard	0,120	0,16	950	840	
	glass fibre guilt	0,047	0,04	12	840	0,18
	cavity	0,029				
	plywood	0,009	0,14	530	900	
	cavity	0,050				0,18
	brickwork	0,105	0,84	1700	800	
Lightweight wall, dynamic		0,072	0,04	40	850	
Heavyweight wall, tight	plaster	0,016	0,26	800	1000	
	concrete block	0,100	0,51	1400	1000	
	urea formaldehyde foam	0,050	0,04	10	1400	0,18
	cavity	0,050				
	brickwork	0,102	0,84	1700	1800	
Heavyweight wall, dynamic		0,145	0,08	400	850	
Lightweight floor	timber flooring	0,025	0,14	650	1200	
	insulation	1,003				25.0
Heavyweight floor	screed	0,050	0,41	1200	840	
	reinforced concrete slab	0,150	0,51	1400	100	
	insulation	1,000				25.0
Roof	asphalt	0,019	0,50	1700	1000	
	fibreboard	0,013	0,06	300	1000	
	air gap	0,025				0,17
	glass fibre guilt	0,100	0,04	12	840	
	plasterboard	0,010	0,16	950	840	
Lightweight internal wall	plasterboard	0,012	0,16	950	840	
	cavity	0,050				0,18
	plasterboard	0,012	0,16	950	840	
Heavyweight internal wall	plaster	0,016	0,26	800	1000	
	concrete block	0,100	0,51	1400	1000	
	plaster	0,015	0,26	800	1000	